THE APOLLO 17 SURFACE ELECTRICAL PROPERTIES EXPERIMENT REVISITED. R.E. Grimm[1], [1]Planetary Science Directorate, Southwest Research Institute, 1050 Walnut St. #300, Boulder, CO, 80302, grimm@boulder.swri.edu

Introduction: The Surface Electrical Properties (SEP) experiment deployed at the Apollo 17 landing site in the Taurus-Littrow valley was a continuous-wave, radiofrequency (1-32 MHz) instrument designed to probe the subsurface from depths of meters to kilometers [1]. Unfortunately, analysis and reporting of the SEP results were very limited, likely due to the difficulty in modeling the interferometric data. Subsequent impulse systems [GPR: ref. 2] offered higher resolution for terrestrial studies without complex modeling. Modern computational methods, as well as new perspectives and spacecraft-mission results for the Moon, invite a new analysis of this pioneering experiment.

Background: Signals were transmitted at six frequencies by orthogonal electric dipoles laid out near the lunar module and three components of the magnetic field were measured on the lunar rover at useful distances up to 1.6 km. Interference between the free-space wave, direct ground wave, and waves reflected from the subsurface form a pattern of peaks and nulls with range. Note that the SEP only recorded power and not signed amplitudes.

The initial rover traverse was nearly perpendicular to one transmitter (Tx) antenna; this is referred to as the broadside configuration and the other antenna as endfire. The maximum energy is radiated from a dipole at 90°, so energy from the broadside antenna varies slowly with azimuth, whereas 0° to a dipole is a null and therefore energy from the endfire antenna is weaker and varies strongly with azimuth. Furthermore, the horizontal components of the received (Rx) magnetic field depend on azimuth. For these reasons, structural modeling by waveform analysis was carried out only for the vertical magnetic field Rx for the broadside Tx, although attenuation was analyzed in all six components. The data were obtained from the NASA Space Science Data Coordinated Archive (NSSDCA).

Attenuation: The gross range decay of the signals was fit by a simple equation combining spherical spreading, first-order interference, and attenuation: $P(\text{dB}) = P_0 - 40 \log r - \alpha r$, where P_0 is a constant, α is the attenuation coefficient (dB/m), and r is the range (m). The loss tangent $\tan\delta \approx 1.1\text{x}10^7 \alpha f/\sqrt{\varepsilon}$, where f is the frequency (Hz) and ε is the dielectric constant, for $\tan\delta << 1$. Keeping only fits where the fractional error in α < 100% (9 of 36), the derived mean loss tangent is 0.0122 and the range is 0.0033 to 0.0179. Most of the retained $\tan\delta$ are for the broadside Tx vertical Rx configuration.

New regression relationships were derived for ε and $\tan\delta$ of lunar samples as functions of density ρ and metal M = %TiO2 +%FeO [compare to 3]. The SEP loss tangents ~0.01 are consistent with laboratory-measured absorption in Apollo 17 basalts. Thus the attenuation in the SEP data can be explained by absorption with negligible small-scale scattering; the latter can be quantified as a dearth of 10-m scale lateral heterogeneity and a mean-free path of kilometers. The subfloor basalt at Taurus-Littrow therefore is largely coherent and presents a laterally uniform, if slightly absorbing, environment at RF wavelengths.

Vertical Structure: Multilayer models for the subsurface dielectric structure were determined by optimizing the parameters that best fit the predictions of a numerical waveform model to the SEP data. The RF module of Comsol Multiphysics® (v. 5.2) was used to calculate frequency-domain wavefields in Transverse Electric (TE) axisymmetry (**Fig. 1**). 2D calculations are fast and axisymmetry produces the required spherical spreading. However, the broadside electric dipole source cannot be directly represented; instead, a vertical magnetic dipole was used, which has the same far-field radiation pattern in the TE plane [e.g., 4]. The model domain comprises an overlying, uniform vacuum layer and a subsurface with vertically varying dielectric constant. Perfectly Matched Layers (PMLs) simulate open boundaries.

The cyclical nature of interference patterns in RF interferometry means that the inverse problem, or estimation of dielectric structure, can be strongly nonunique. In order to better seek the global best solutions, an initial Monte Carlo (MC) search was followed by Particle Swarm (PS) optimization. MC simply randomly selects parameters from specified ranges, whereas PS propagates multiple models toward a best solution [5]. The inversion was regularized by specifying 13 log-spaced interfaces to a maximum depth of 2 km and further requiring that the dielectric constant (which maps directly to density [6]) increases with depth.

The coefficient of determination R^2 = 0.65 to 0.85 for the best-fit models at each frequency 1-16 MHz (**Fig. 2**. what happened to 32 MHz). Joint inversion over all frequencies performed poorly, so instead a cooperative result was formed by averaging the individually derived structures.

Discussion: The composite model shows a sharp decrease in porosity in the top 20–30 m, with little change below 300 m (**Fig. 3**). This likely tracks the transition

from fully gardened regolith, to impact-fractured rock, to largely intact 3.7-Ga basalt. The bottom of the basalt was not detected by the SEP to a depth of ~2 km or more, which is consistent with reanalysis of Apollo 17 seismic and gravity data.

Densities recovered from the SEP approach those of solid rock at depth and reflect volcanic fill characteristic of maria instead of highlands megaregolith and so cannot be readily compared to the GRAIL-derived porosity map [11]. A future SEP-like experiment would give superior penetration available at low frequency compared to the higher frequencies required for orbital operations.

References: [1] Simmons G. et al. (1973) in *NASA SP-330*, Ch. 15. [2] Annan A.P. and Davis J.L. (1976) *Radio Sci.*, *11*, 383. [3] Carrier W.D. et al. (1991) in *Lunar Sourcebook*, Cambridge Univ. Press. [4] Balanis C.A. (1997) *Antenna Theory*, Wiley & Sons. [5] Kennedy J. (2011) in *Encyclopedia of Machine Learning*, Springer. [6] Olhoeft G. and Strangway D.W. (1975) *EPSL 24*, 394. [7] Kiefer W. et al. (2012) *GRL, 39*, 2012GL051319. [8] Kovach R.L. et al. (1973) in *NASA SP-330*, Ch 10. [9] Cooper M.R. et al. (1974) *Rev. Geophys. 12*, 291. [10] Heffels A. et al. (2017) *PSS 135*, 43. [11] Wieczorek M. et al. (2013) *Science, 339*, 671.

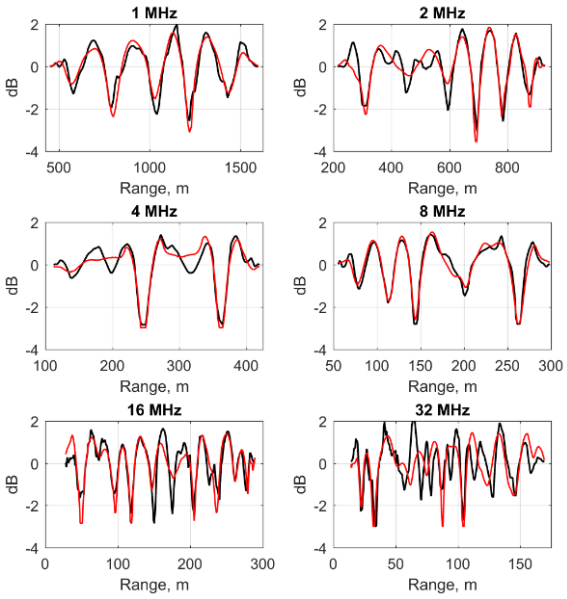

Fig. 2. Numerical computations of SEP interference patterns for best-fitting stepwise models (red) compared to SEP data (black).

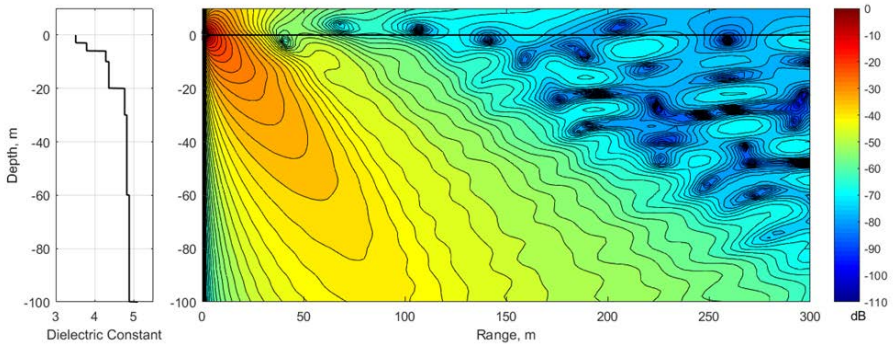

Fig. 1. Computed SEP out-of-plane electric field power at 8.1 MHz (right) for best-fitting (Fig. 2) layered dielectric structure (left) at this frequency. Note radiation of most of the signal into the subsurface and well-developed interference patterns away from the transmitter, especially at the surface.

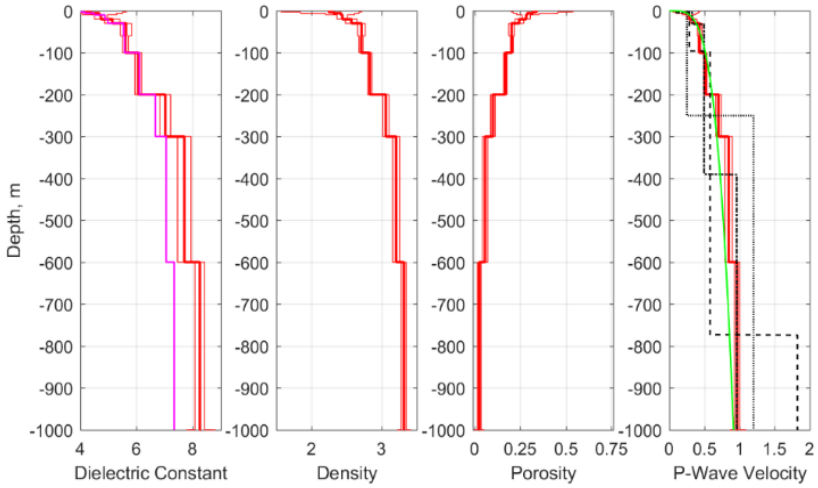

Fig. 3. Depth profiles and 1-σ error bounds for average of individual-frequency SEP inversions (red) vs joint inversion (magenta). Dielectric constant is converted to density using formula specific to Taurus-Littrow samples, $\varepsilon = 1.89^{\rho}$. Porosity follows by assuming grain density 3.4 Mg m^{-3} [7]. P-wave velocity scaled as $v = v_1\rho^4$ (Gardner's relation using v_1 = 8 ms^{-1}), compared to various interpretations of seismic data (black dot–ref. 8; black dash-dot–ref 9; black dash 10; green – ref 9, continuous model).